Solutions of nonplanar KP-equations for dusty plasma system with GE-method

S. Reyad, M. M. Selim, A. EL-Depsy, and S. K. El-Labany

Citation: Physics of Plasmas **25**, 083701 (2018); doi: 10.1063/1.5026616
View online: https://doi.org/10.1063/1.5026616
View Table of Contents: http://aip.scitation.org/toc/php/25/8
Published by the American Institute of Physics

Solutions of nonplanar KP-equations for dusty plasma system with GE-method

S. Reyad, M. M. Selim, A. EL-Depsy, and S. K. El-Labany
Department of Physics, Faculty of Science, Damietta University, New Damietta, P. O. 34517, Egypt

(Received 21 February 2018; accepted 2 July 2018; published online 30 July 2018)

The propagation of three-dimensional nonlinear dust acoustic waves in a dusty plasma consisting of positive and negative dust grains as well as Boltzmann distributed electrons and ions is investigated. Using a reductive perturbation method, Cylindrical Kadomtsev-Petviashvili and Spherical Kadomtsev-Petviashvili equations, appropriate for describing the evolution of the system, are derived. The Generalized Expansion method is used to find the various solutions of the obtained nonlinear Kadomtsev-Petviashvili equations. New classes of triangular, hyperbolic solitary, rational, and Jacobi elliptical type solutions are obtained and graphically presented. It is found that the proposed dusty plasma model can support solitary waves with compressive and rarefactive potential pulses. Moreover, the effects of plasma parameters on this solitary wave structure are investigated. The current findings are applied to a cosmic-type plasma in different regions of space, viz. cometary tails, mesosphere, and Jupiter's magnetosphere as well as laboratory-type plasma such as low temperature experiments, where a dusty plasma with opposite polarity is dominant. *Published by AIP Publishing.* https://doi.org/10.1063/1.5026616

I. INTRODUCTION

The dusty plasma (DP) usually consists of micro-sized dust grains with positive and negative charges as well as neutral particles beside electrons and ions. This type of plasma was first predicted by the theoretical model of Rao *et al.*[1] Since then, the DP has received a great deal of interest because of its vital role in explaining many astrophysical and space phenomena.[2–18] It should be mentioned also that the DP has a significant impact in the laboratory experiments.[19–23]

The DP is encountered in different regions of space environments, such as lower and upper mesospheres, planetary rings, cometary tails, and comae, interplanetary spaces, Martian atmosphere, and at the Moon surface.[6,9,13,15–17] In laboratory, the DP occurs in low temperature plasmas during plasma processing (e.g., in microelectronics) and is also artificially created in plasma discharges, plasma coating, radio-frequency discharges, tokamaks, etc.[10,24] Due to these interesting applications of dusty plasmas in several areas of science and technology, the research on dusty plasmas has increased day by day.[2–20]

The charging processes of the dusty plasma are divided into negative charging by plasma electrons and ion currents as well as positive charging by secondary electron emission, UV radiations, inhomogeneous thermionic emission, etc.[7,10,25] However, negative charging is the dominant process due to the high mobility of electrons. Many investigations have shown the presence of both positively and negatively charged dust in various regions of space and astrophysical environments.[10,13]

The propagation of dust acoustic waves (DAWs) in plasma is governed by two types of nonlinear partial differential equations (NLPDEqs). These equations are: (*i*) NLPDEqs with constant coefficients: for which many direct methods have been used to solve them such as the inverse scattering method,[26] sine-cosine method,[27] tanh function method,[28,29] Jacobi elliptic function expansion method,[30–32] etc…. (*ii*) NLPDEqs with variable coefficients: for which the solution methods are limited and most of the aforementioned ones are restricted to the constant coefficient models. We can mention here that the generalized G'/G-expansion method is one of the most interesting methods to solve the NLPDEqs with variable coefficients. Zhang *et al.*[33] applied the G'/G-expansion method to solve the modified Korteweg-de Vries (mKdV) equation with variable coefficients and they have obtained hyperbolic, trigonometric, and rational solutions. The G'/G-expansion method is used by the authors to solve the nonlinear Cylindrical Kadomtsev-Petviashvili (CKP) equation with variable coefficients, for a system of dusty plasma with Maxwellian distributed ions and electrons.[34] New classes of hyperbolic, geometrical, and rational solutions are obtained.

The nonlinear propagation of DAWs in a strongly coupled inhomogeneous dusty plasma is studied by Alinejad and Mamun[35] for a plasma system consisting of strongly correlated negative charged dust grains and weakly correlated electrons and ions. The evolution equation for this system is a variable coefficient KdV equation with additional terms due to the density gradient. The solution of this equation is found by appropriate transformations. El-Taibany *et al.*[36] and El-Labany *et al.*,[37] studied the modified Zakharov-Kuznetsov (ZK) equations for an inhomogeneous dusty plasma system with constant and fluctuating dust charge. These equations are nonlinear equations with variable coefficients and describe the nonlinear propagation of DAWs in such plasma systems. They used special transformations to reduce the variable coefficient modified ZK equation to a constant coefficient one. Then, this equation is solved by the traditional methods.

The aim of this work is finding the analytical solutions of two interesting classes of variable coefficients NPDEqs that govern the evolution of many multi-component plasma systems: the CKP and Spherical Kadomtsev-Petviashvili (SKP) equations.[18,38–41] These equations describe the basic properties of the acoustic waves propagation in three dimensional nonplanar geometry plasma systems. To solve the two considered KP equations (CKP and SKP), we used the Generalized Expansion (*GE*)–method, developed by Sabry *et al.*[42] The obtained solutions include solitary wave solutions besides Jacobi and Weierstrass doubly periodic wave solutions.

In this paper, we used the *GE*-method, explained in the Appendix, to solve the CKP and SKP equations for a four component dusty plasma system consisting of positive dust, negative dust, Boltzmann distributed electrons, and ions. In Sec. II, the basic equations of the plasma system are given and reduced to the CKP and SKP equations by the reductive perturbation method (RPM).[43] In Sec. III, the *GE*-method is applied to obtain the various solutions of these equations. Section IV is devoted to the investigation of the basic characteristics of the obtained solutions for laboratory-type and cosmic-type DPs. Finally, the discussion and conclusions are presented.

II. NONPLANAR KP EQUATIONS

In this work, we consider an unmagnetized, collisionless, four-component dusty plasma system. A collisionless plasma system means that the mean free path between collisions of plasma particles (electrons, ions,…) must be much larger than the typical macroscopic length scale over which the plasma quantities vary. Hence, the collision frequencies are much smaller than the typical plasma frequency. This type of plasma is found in space, where plasmas often have very low densities.[24,44] In addition, we consider a plasma system consisting of positive and negative dust grains as fluids and a background of ions and electrons. The dust grains are strongly correlated with each other due to their lower temperature and higher electric charge, whereas both the electrons and ions are weakly correlated due to their higher temperatures and lower electric charges.[45–47] Furthermore, the phase velocity of the DAW is much smaller than the electron and ion thermal speeds. Accordingly, the electrons and ions establish equilibrium in the DAW potential. Here, the pressure gradient is balanced by the electric force, leading to Boltzmann distributed electrons and ions.[48,49] Hence, the four constituents of our system are positive and negative dust grains in addition to Boltzmann distributed electrons and ions. The dynamics of this system are governed by the following continuity, momentum and Poisson equations

$$\frac{\partial n_\pm}{\partial t} + \nabla.(n_\pm \mathbf{u}_\pm) = 0, \tag{1}$$

$$\left(\frac{\partial}{\partial t} + \mathbf{u}_+.\nabla\right) u_+ = -\alpha\beta\,\nabla\phi, \tag{2}$$

$$\left(\frac{\partial}{\partial t} + \mathbf{u}_-.\nabla\right) u_- = \nabla\phi, \tag{3}$$

$$\nabla^2\phi = n_e - n_i - n_+ + \alpha n. \tag{4}$$

Furthermore, the electron and ion distributions are given by

$$n_e = \mu_e \exp(\sigma\phi), \quad n_i = \mu_i \exp(-\phi). \tag{5}$$

In Eqs. (1)–(5), $n_\pm$ and $u_\pm$ are the positive/negative dust fluid densities and velocities, respectively, and ϕ is the electrostatic potential. $\sigma = T_i/T_e$, where T_e and T_i are the electron and ion temperature, respectively. $\mu_e = \frac{n_{e0}}{z_- n_{-0}}$ and $\mu_i = \frac{n_{i0}}{z_- n_{-0}}$, where n_{i0} and n_{e0} are the unperturbed ion and electron densities. $\beta = m_-/m_+$ and $\alpha = Z_+/Z_-$ are the dust mass and dust charge ratios, where $m_+, m_-, Z_+,$ and Z_-, are the positive and negative dust masses and charge numbers, respectively.

The densities $n_\pm$, n_i, and n_e are normalized by the unperturbed negative dust density, n_{-0-}. The velocity vector, $u_\pm$, is normalized by $C_s = (Z_- k_B T_i/m_-)^{1/2}$, while the electrostatic potential ϕ is normalized by $k_B T_i/e$. The space and time variables are scaled by the negative dust Debye radius, $\lambda_{D-} = (Z_- k_B T_i/4\pi Z_-^2 e^2 n_{-0})^{1/2}$ and the negative dust plasma period, $\omega_{p-} = (4\pi Z_-^2 e^2 n_{-0}/m_-)^{1/2}$, respectively. Although the distributions of electrons and ions are taken as Boltzmann, the argument of this work can be generalized to various systems, having non-Maxwellian distributions. The neutrality property of this plasma system implies

$$\mu_i - \mu_e + \alpha Q = 1, \tag{6}$$

where $Q = \frac{n_{+0}}{n_{-0}}$.

To investigate the nonlinear propagation of the electrostatic DAWs in the considered plasma system, the RPM is employed. This method is used to convert the coupled nonlinear Eqs. (1)–(5) into a single nonlinear evolution equation for the electrostatic potential, ϕ. According to the RPM, the independent variables in Eqs. (1)–(5) can be stretched in a new frame as

$$\begin{aligned} &R = \epsilon^{1/2}(r - \lambda t), \quad \Theta = \epsilon^{-1/2}\theta, \\ &Z = \epsilon z, \quad \varphi = \varphi \quad \text{and} \quad T = \epsilon^{3/2} t, \end{aligned} \tag{7}$$

where $\epsilon < 1$, is a small positive parameter and λ is the frame speed. R, Θ, φ, and Z are the radial, angular, azimuthal, and axial coordinates. Furthermore, the dependent variables can be expanded as

$$\begin{aligned} n_\pm &= \rho + \epsilon n_{\pm-}^{(1)} + \epsilon^2 n_{\pm-}^{(2)} + \cdots, \\ u_\pm &= \epsilon u_{\pm-}^{(1)} + \epsilon^2 u_{\pm-}^{(2)} + \cdots, \\ v_\pm &= \epsilon^{3/2} v_\pm^{(1)} + \epsilon^{5/2} v_\pm^{(2)} + \cdots, \\ w_\pm &= \epsilon^{3/2} w_\pm^{(1)} + \epsilon^{5/2} w_\pm^{(2)} + \cdots, \\ \phi &= \epsilon\phi^{(1)} + \epsilon^2\phi^{(2)} + \cdots, \end{aligned} \tag{8}$$

where $\rho = Q$ for positive dust density and $\rho = 1$ for negative dust density. $u_\pm$ and $v_\pm$ are the positive/negative velocities in r, θ directions, while $w_\pm$ is the positive/negative velocity in the z direction for cylindrical and φ direction for spherical coordinates, respectively. Substituting the stretched variables, Eq. (7) and the expansions, Eqs. (8) into Eqs. (1)–(5), we can isolate distinct orders in ϵ. The first and the second order equations in ϵ lead to the KP equations. In the cylindrical coordinates, the CKP equation for $\phi(R, \Theta, Z, T)$ is derived as

$$\frac{\partial}{\partial R}\left(\frac{\partial\phi}{\partial T}+\frac{\phi}{2T}+A\phi\frac{\partial\phi}{\partial R}+B\frac{\partial^3\phi}{\partial R^3}\right)+\frac{1}{2\lambda T^2}\frac{\partial^2\phi}{\partial\Theta^2}+\frac{\lambda\partial^2\phi}{2\,\partial Z^2}=0. \tag{9}$$

Similarly, in the spherical coordinates SKP for $\phi(R, \Theta, \varphi, T)$ is derived as

$$\frac{\partial}{\partial R}\left(\frac{\partial\phi}{\partial T}+\frac{\phi}{T}+A\phi\frac{\partial}{\partial R}\phi+B\frac{\partial^3\phi}{\partial R^3}\right)+\frac{1}{2\lambda^2T^2}\left(\frac{\partial\phi^{2(1)}}{\partial\Theta^2}+\frac{1}{\Theta}\frac{\partial\phi}{\partial\Theta}+\frac{1}{\Theta^2}\frac{\partial^2\phi}{\partial\varphi^2}\right)=0. \tag{10}$$

The frame speed, λ, and the coefficients, A and B, are given by

$$\lambda=\sqrt{\frac{\alpha^2\beta Q+1}{\mu_i+\mu_e\,\sigma}}, \tag{11}$$

$$A=B\left[\frac{3Q\alpha^3\beta^2}{\lambda^4}-\frac{3}{\lambda^4}-\mu_e\,\sigma^2+\mu_i\right], \tag{12}$$

and

$$B=\left[\frac{\lambda^3}{2[1+\alpha^2\beta Q]}\right]. \tag{13}$$

For the derivation details of CKP and SKP equations (9) and (10), the reader refers to Refs. 18 and 40, given by one of the authors.

III. SOLUTIONS OF CKP AND SKP EQUATIONS

To get the analytical solutions of the CKP and SKP Eqs. (9) and (10), we apply the *GE*-method, presented in the Appendix. According to this method, we can express the solution of these equations as a polynomial given by Eq. (A2). Balancing the highest derivative term with the non-linear term in both Eqs. (9) and (10) leads to $m=2$. Hence, Eq. (A2) is reduced to

$$\phi(\zeta)=A_0(\Theta,T)+A_1(\Theta,T)\omega(\zeta)+A_2(\Theta,T)\omega(\zeta)^2, \tag{14}$$

where $\omega(\zeta)$ is given by Eq. (A4) and $\zeta=\alpha(T)R+\beta(T)Z+\delta(\Theta,T)T$. Substituting Eq. (14) along with Eq. (A4) into Eqs. (9) and (10), then setting the coefficients of ω^i and $\omega^i\sqrt{\sum_{j=0}^{4}c_j\,\omega^j}$ (where $i=0-6$) to zero, we get a system of over-determined partial differential equations with respect to the unknown functions $A_0(\Theta,T)$, $A_1(\Theta,T)$, $A_2(\Theta,T)$, $\alpha(T)$, $\beta(T)$, $\delta(\Theta)$. Solving the obtained system for $c_1=c_3=0$, we get

$$\alpha(T)=\alpha_0,\quad \beta(T)=\beta_0,\quad A_1(\Theta,T)=0,$$
$$A_2(\Theta,T)=-\frac{12\,B\,c_4\,k^2\alpha_0^2}{A}. \tag{15}$$

The coefficients, $A_0(\Theta, T)$ and $\delta(\Theta, T)$, for the CKP equation are derived as

$$A_0(\Theta,T)=-\frac{c^2+\lambda\,(2u_0\,\alpha_0+8B\,c_2\,k^2\alpha_0^4+\lambda\,\beta_0^2)}{2A\,\alpha_0^2\,\lambda}, \tag{16}$$

$$\delta(\Theta,T)=u_0-\frac{1}{2}\lambda\,\alpha_0\,\Theta^2+c\,\Theta, \tag{17}$$

whereas for the SKP equation, we get

$$A_0(\Theta,T)=-\frac{1}{2A\,\alpha_0^2\lambda^2\Theta^2T^2}\times\left(\begin{array}{l}\beta_0^2+c^2T^2-2u_0\alpha_0\lambda^2\Theta^2T^2-2c\alpha_0\lambda^2\Theta^2T^2\\+8Bc_2\alpha_0^4\lambda^2\Theta^2T^2+2c\alpha_0\lambda^2\Theta^2T^2\log(\Theta)\end{array}\right), \tag{18}$$

$$\delta(\Theta,T)=-u_0-\frac{1}{2}\alpha_0\lambda^2\Theta^2+c\,\log(\Theta), \tag{19}$$

where, α_0, β_0, c, and u_0 are arbitrary constants.

Substituting the values of $\omega(\zeta)$, from Eqs. (A5) to (A12), in Eq. (14) gives the solutions for CKP and SKP equations. These solutions (differ in the values of $A_0(\Theta, T)$ and $\delta(\Theta, T)$) are summarized as follows:

$$\phi_1=A_0(\Theta,T)-\frac{c_2}{c_4}A_2(\Theta,T)\mathrm{sech}^2\left[\sqrt{c_2}\zeta\right],$$
$$c_0=0\quad c_2>0,\ c_4<0, \tag{20}$$

$$\phi_2=A_0(\Theta,T)-\frac{c_2}{2c_4}A_2(\Theta,T)\tanh^2\left[\sqrt{\frac{-c_2}{2}}\zeta\right],$$
$$c_0=\frac{c_2^2}{4c_4}\quad c_2<0, c_4>0, \tag{21}$$

$$\phi_3=A_0(\Theta,T)-\frac{c_2}{c_4}A_2(\Theta,T)\sec^2\left[\sqrt{-c_2}\zeta\right],$$
$$c_0=0\qquad c_2<0, c_4>0, \tag{22}$$

$$\phi_4=A_0(\Theta,T)+\frac{c_2}{c_4}A_2(\Theta,T)\tan^2\left[\sqrt{c_2}\zeta\right],$$
$$c_0=0\quad c_2<0, c_4>0, \tag{23}$$

$$\phi_5=A_0(\Theta,T)+\frac{A_2(\Theta,T)}{\sqrt{c_4}\zeta^2},\ \ c_0=c_2=0,\ \ c_4\succ0, \tag{24}$$

$$\phi_6=A_0(\Theta,T)-\frac{c_2\,m^2A_2(\Theta,T)cn^2\left[\sqrt{\frac{c_2}{2m^2-1}}\zeta\right]}{c_4(2m^2-1)},$$
$$c_2>0,\ c_4>0,\quad c_0=-\frac{c_2^2m^2(1-m^2)}{c_4(2m^2-1)^2}, \tag{25}$$

$$\phi_7=A_0(\Theta,T)-\frac{c_2\,m^2A_2(\Theta,T)sn^2\left[\sqrt{\frac{-c_2}{1+m^2}}\zeta\right]}{c_4(1+m^2)},$$
$$c_2>0,\ c_4<0,\quad c_0=-\frac{c_2^2(1-m^2)}{c_4(2-m^2)^2}, \tag{26}$$

$$\phi_8=A_0(\Theta,T)-\frac{c_2\,A_2(\Theta,T)dn^2\left[\sqrt{\frac{c_2}{2-m^2}}\zeta\right]}{c_4(m^2-2)},$$
$$c_2<0,\ c_4>0,\quad c_0=-\frac{c_2^2m^2}{c_4(m^2+1)^2}, \tag{27}$$

where m is the modulus of the three Jacobi elliptic functions cn, dn, and sn. For $m \to 0$, the Jacobi elliptic functions degenerate into their corresponding triangular functions, i.e., $sn(x) \to \sin(x)$ and $cn(x) \to \cos(x)$. For $m \to 1$, the Jacobi elliptic functions degenerate into the hyperbolic functions, i.e., $sn(x) \to \tanh(x), cn(x) \to \mathrm{sech}(x)$. Therefore, solution ϕ_6 degenerates into the solitary wave solution ϕ_1 and ϕ_7 degenerates to the solitary wave solution

$$\phi_9 = A_0(\Theta, T) - \frac{c_2 A_2(\Theta, T)\tanh^2\left[\sqrt{-\frac{c_2}{2}}\zeta\right]}{2c_4}. \tag{28}$$

Since α_0, β_0, c_2, and c_4 are arbitrary constants, we can take $c_2 = \frac{\lambda\beta_0^2 - 2u_0\alpha_0}{4B\alpha_0^4}$. We may also set $c = 0$, since the transverse perturbation should be weak from the physical view point. Hence, the solitary solution, (28), after substitution of $A_2(\Theta, T)$, $A_0(\Theta, T)$ and $\delta(\Theta, T)$ from Eqs. (15)–(17) for the CKP equation, is reduced to the equation

$$\phi = \phi_0 \,\mathrm{sech}^2\left[\frac{\alpha_0 R + \beta_0 Z + \left(u_0 - \frac{1}{2}\alpha_0\lambda\Theta^2\right)T}{W}\right], \tag{29}$$

where the amplitude, ϕ_0, and the width, W, of the ion-acoustic solitary wave are given by

$$\phi_0 = -\frac{3\left(2u_0\alpha_0 - \beta_0^2\lambda\right)}{2A\alpha_0^2}, \tag{30}$$

$$W = \sqrt{\frac{8B\alpha_0^4}{\beta_0^2\lambda^2 - 2u_0\alpha_0}}. \tag{31}$$

In a similar way, for the SKP equation we can take the arbitrary constants; $c = 0, \beta_0 = 0$, $c_2 = \frac{u_0}{4B\alpha_0^3}$. Hence, the solitary solution, (28), after substitution of $A_2(\Theta, T)$, $A_0(\Theta, T)$, and $\delta(\Theta, T)$ from Eqs. (15), (18), and (19), is reduced to

$$\phi = \phi_0 \,\mathrm{sech}^2\left[\frac{\alpha_0 R - \left(u_0 + \frac{1}{2}\alpha_0\lambda\Theta^2\right)T}{W}\right], \tag{32}$$

where

$$\phi_0 = \frac{3u_0}{A\alpha_0}, \quad \text{and} \quad W = \sqrt{\frac{4B\alpha_0^3}{u_0}}. \tag{33}$$

Here, ϕ_0 is the amplitude and W is the width of the ion-acoustic solitary wave in spherical geometry.

IV. NUMERICAL RESULTS

In this section, we graphically investigate the solutions of the SKP equation to verify the validity of the *GE*-method. A similar numerical analysis is presented in our paper, Ref. 34, for the solutions of the CKP equation, obtained by the $G'/G-$ expansion method. The same solutions are obtained in this regard with the *GE*-method with a proper choice of the free parameters. So we do not need to represent the CKP solutions graphically here. It is interesting to notice that the obtained solutions are hyperbolic solitary (ϕ_1, ϕ_2, ϕ_9), triangular (ϕ_3, ϕ_4), rational (ϕ_5), and Jacobi elliptical ($\phi_6 - \phi_8$) type solutions.

In these numerical results, we consider a laboratory and a cosmic-type DP. For a laboratory-type DP, we mention here some conditions under which both positively and negatively charged dust grains can be produced. Assume that dust grains with an equal size are immersed in a plasma of density N and with ion and electron thermal speeds, C_i and C_e, respectively. Also assume that the grains are of two different types (one is metallic with a photoemission efficiency, $\eta \simeq 1$, and the other is dielectric with $\eta \simeq 0.1$, for example) are subjected to photon flux, P. For any isolated grain, the total charging current is zero. If the potential of a grain relative to the plasma is ϕ_s, then we have[22]

$$-C_e\, e^{\frac{e\phi_s}{k_B T_e}} + C_i\left(1 - \frac{e\phi_s}{k_B T_i}\right) + \eta\frac{P}{N} = 0, \quad \text{for } \phi_s < 0, \tag{34}$$

and

$$-C_e\left(1 + \frac{e\phi_s}{k_B T_e}\right) + C_i e^{-\frac{e\phi_s}{k_B T_i}} + \eta\frac{P}{N} = 0, \quad \text{for } \phi_s > 0. \tag{35}$$

For a plasma with $T_e = 2\,\mathrm{eV}$, $T_i = 0.2\,\mathrm{eV}$, and $m_i = 6.7\times10^{-26}\,\mathrm{kg}$, these two equations allow calculating $\frac{e\phi_s}{k_B T_e}$ in terms of the ratio $\frac{P}{N}$, for $\eta \simeq 0.1$ and $\eta \simeq 1$. It is found that, in the range $7\times10^5\,\mathrm{m/s} \le \frac{P}{N} \le 5\times10^6\,\mathrm{m/s}$, a plasma with positive and negative dust grains of density $8\times10^{15}\,\mathrm{m}^{-3} \le N \le 6\times10^{16}\,\mathrm{m}^{-3}$ is created at photon flux, $P \simeq 4\times10^{22}\,\mathrm{m}^{-2}\mathrm{s}^{-1}$.[7] These density values are in the range of several types of laboratory plasmas.

Under the experimental conditions illuminated above, we adopt a specific set of real parameters values for a laboratory-type DP. We consider the example of a laboratory produced dusty plasma that was addressed by D'Angelo[22] and El-Taibany *et al.*[23] Table I. For the sake of comparison, a cosmic-type dusty plasma which is related to the polar mesospheric summer echoes (PMSE),[21] is considered. The parameters of our model, corresponding to each case, are evaluated and presented in Table I. In both cases, we have made use of the neutrality condition, in order to calculate the positive to the negative dust number density ratio, Q.

It is clear from the table that the parameters values for the laboratory-type DP are different from those for the cosmic-type DP. In the laboratory-type DP, the mass and charge of positive and negative dusts are in the same order of magnitude, while for the cosmic-type DP the mass and charge for negative dusts are much larger than positive ones. Furthermore, the thermal speed of negative dust, C_-, is much smaller than the positive one, C_+. In both cases, the ion and electron temperatures are in the same order of magnitude ($\sigma = \frac{T_i}{T_e} \simeq 1$). We may infer the high values of the charge ratio in cosmic-type plasma situations to ion drifts of $\sim$320 km/s which are large enough to excite both dust-acoustic modes. Ion drifts of several hundreds of km/s are in the order of solar wind speeds. Furthermore, the dust species

TABLE I. Laboratory and cosmic-type plasma parameters presented in Ref. 22 and their corresponding calculated parameters in the current model.

Cosmic-type plasma		Laboratory-type plasma	
Reference 22	Current model	Reference 22	Current model
$m_i = 1.67 \times 10^{-27}$ kg	$Q = 100$	$m_i = 6.7 \times 10^{-26}$ kg	$Q = 0.125$
$m_+ = 4 \times 10^{-21}$ kg	$\mu_e = 4.995$	$m_+ = 2 \times 10^{-18}$ kg	$\mu_e = 1.188$
$m_- = 4 \times 10^{-15}$ kg	$\mu_i = 4.995$	$m_- = 2.3 \times 10^{-18}$ kg	$\mu_i = 2.08$
$Z_+ = 70$	$\sigma = 0.997$	$Z_+ = 5$	$\sigma = 1.04$
$Z_- = 7000$	$\beta = 10^6$	$Z_- = 6$	$\beta = 1.15$
$C_+ = \sqrt{\frac{k_B T_+}{m_+}} = 0.6$ m/s	$\alpha = 0.01$	$C_+ = 8.94 \times 10^{-2}$ m/s	$\alpha = 0.833$
$C_- = \sqrt{\frac{k_B T_-}{m-}} = 6 \times 10^{-4}$ m/s		$C_- = 8.94 \times 10^{-2}$ m/s	
$C_i = \sqrt{\frac{k_B T_i}{m_i}} = 3 \times 10^4$ m/s		$C_i = 450$ m/s	
$C_e = \sqrt{\frac{k_B T_e}{m_e}} = 1.3 \times 10^6$ m/s		$C_e = 1.2 \times 10^5$ m/s	
$\varepsilon_- = \frac{n_{-0}}{n_{i0}} = 2.86 \times 10^{-3}$		$\varepsilon_- = 0.08$	
$\varepsilon_+ = \frac{n_{+0}}{n_{i0}} = 2.86 \times 10^{-3}$		$\varepsilon_+ = 0.002$	

masses (solid particles, ice, ….) in cosmic plasma are so much larger than dust masses for the laboratory plasma. However, the negative dusty plasma mode produces extremely low frequency waves, since the negative dust grains are so much more massive than positive dust ($\beta = \frac{m_-}{m_+} \simeq 10^6$) in the cosmic-type plasma. This makes the dynamics of the positive dust pretty much obsolete with respect to the negative ones.

We may now proceed by showing the spatial behaviors, Fig. 1, of the various solutions of the SKP equation, as given by Eqs. (20)–(28), at a specific time. From the graphs, one can divide the profile of the electrostatic potential into three classes; positive(compressive) sinusoidal type DA pulses, Fig. 1(a), negative (rarefactive) sinusoidal DA pluses, Fig. 1(b), and a periodical explosive or blowup solution as shown in Fig. 1(c). The origin of compressive and rarefactive sinusoidal-type DA pulse can be explained as follows; the coefficient of the nonlinear term, A, in the SKP equation, given by Eq. (12), depends on the plasma parameters, Q, σ, α, μ_e, μ_i, and β. At certain values of these parameters, the coefficient of the nonlinear term vanishes ($A = 0$) and the solitary wave is not defined, see Fig. 2(a). For $A > 0$, a compressive pulse (hump) appears, Fig. 1(a), while for $A < 0$ a rarefactive (dip) is obtained, Fig. 1(b). It is important to mention that if we neglect the presence of a positive dust component, i.e., $\alpha = 0$ or $\alpha \ll 1$ as in the cosmic-type DP, we find that A is always positive. This means that only the compressive solitary potential profile exists which is in agreement with the result obtained by Mamun[8] and D'Angelo.[22]

Additionally, the solution, ϕ_2, is a sinusoidal-type periodical solution, which develops a singularity at a finite point,

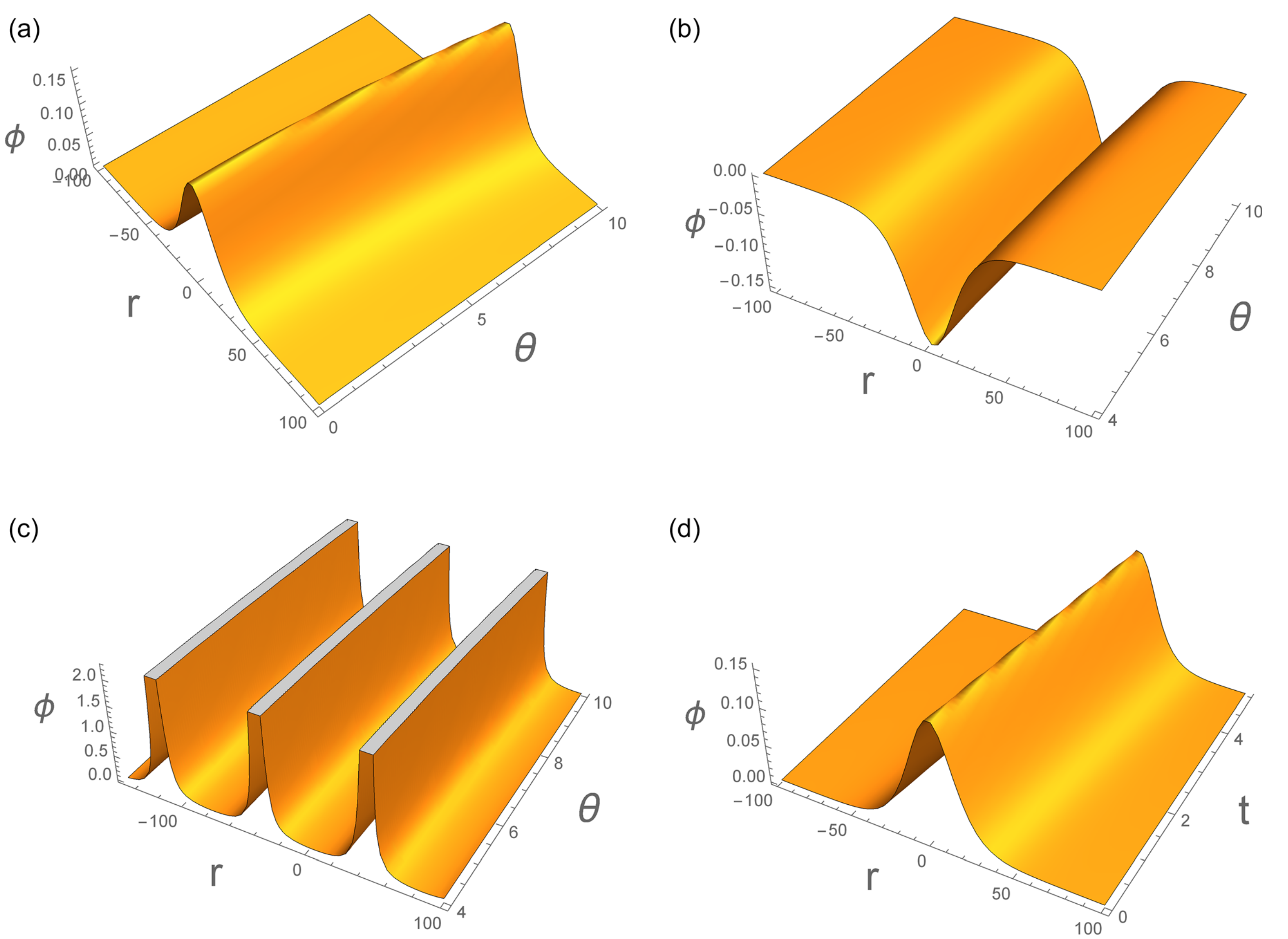

FIG. 1. Three-dimensional graphical representations of the SKP solutions ϕ (r, θ, t): (a) positive(compressive) sinusoidal type solution, (b) negative (rarefactive) sinusoidal solution, (c) periodical explosive or blowup solution and (d) time evolution of the solitary electrostatic potential, $\phi_1(r, \theta, t)$, for the laboratory-type DP.

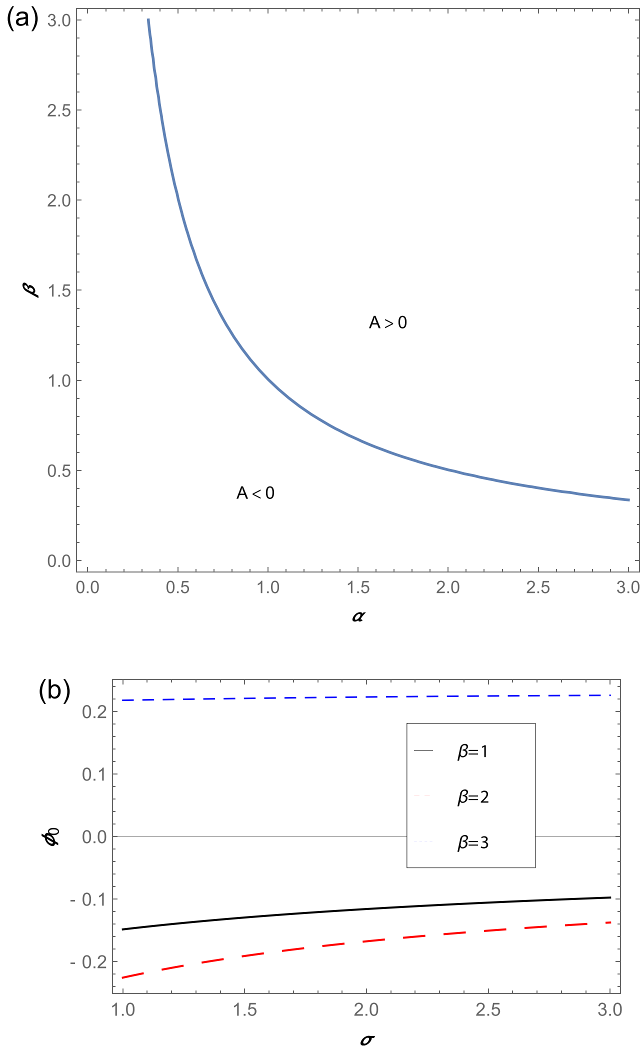

FIG. 2. The coefficient of nonlinear term vanishing curve, $A = 0$ vs. β and α, (b) the variation of compressive ($\phi_0 > 0$) and rarefactive ($\phi_0 < 0$) solitary wave amplitude with plasma parameter, $\sigma(=\frac{T_i}{T_e})$ for the laboratory-type DP, at different values of $\beta(=\frac{m_-}{m_+})$ for the solitary solution represented by Eq. (32).

i.e., for a fixed time this solution blows up at certain values of the angular variable, θ, Fig. 1(c). This potential excitation blowup indicates that an instability in the system may occur due to the effect of nonlinearity. In other words, the variations of plasma parameters disturb the balance between the dispersion and nonlinearity of the system which may destroy the localized excitation stability and lead to an increase in the electrostatic potential amplitude to very high values.[50] The explosive/blowup potential, ϕ_2 and the rational-type potential, ϕ_5, may be helpful for explaining many physical phenomena. The evolution of the electrostatic potential with time, at a specific angular direction, has a similar behavior. In Fig. 1(d), we plot the 3D time evolution of the solitary electrostatic potential, ϕ_1, for the sake of clarification. Such behaviors cannot be noticed in one dimensional problems.

The solitonic type solutions (ϕ_1, ϕ_6, and ϕ_9) are interesting solutions and describe the electrostatic pulses in many plasma systems. They result from the balance between nonlinearity and dispersion forces which may occur at certain values of plasma parameters. It is reasonable to investigate the influences of these parameters on the electrostatic solitary

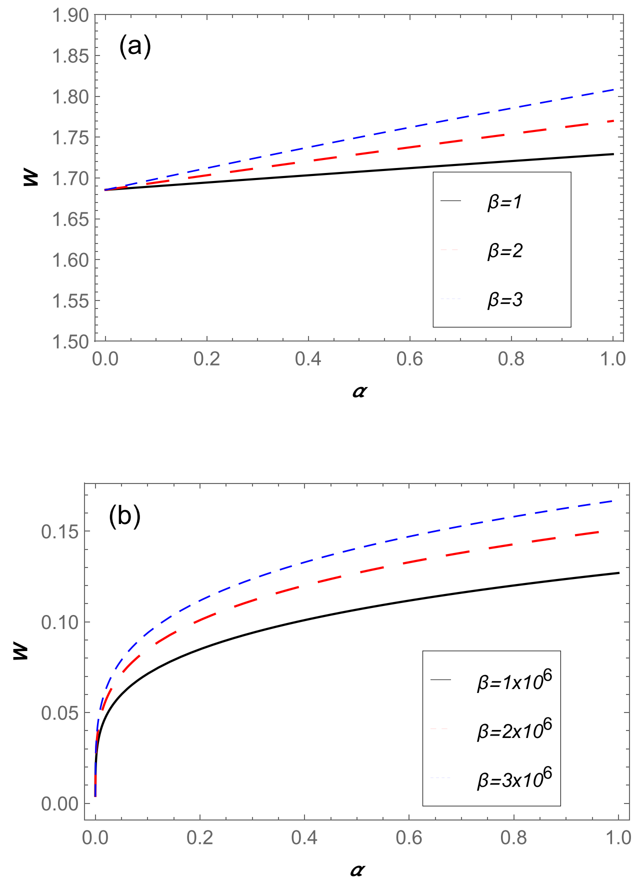

FIG. 3. The variation of the solitary wave width, W, with plasma parameter, $\alpha\left(=\frac{Z_+}{Z_-}\right)$ for: (a) for laboratory-type DP and (b) cosmic-type DP, at different values of $\beta\left(=\frac{m_-}{m_+}\right)$ for the solitary solution represented by Eq. (32).

potential profile, $\phi_1(r, \theta, t)$, represented by Eq. (32). This solitary solution is characterized by the amplitude, ϕ_0, and the width, W, given by Eq. (33). Figure 2(a) displays the $A = 0$ curve for the laboratory-type DP which indicates that the positive (negative) solitary potential profile for the parameters whose values lie above (below) the $A = 0$ curve is obtained. We have also shown graphically how the amplitude, ϕ_0, of the positive and negative solitary potential profiles varies with σ for different values of β. We note that increasing σ leads to an increase in ϕ_0 (taller solitons) for rarefactive ($\beta < 3.63$) and compressive ($\beta > 3.63$) pulses.

Figures 3–5 show the dependence of W on α, μ_i, and β. The numerical values of these parameters that we chose in numerical analysis are relevant to the laboratory-type DP [(a) panel of the figures] and cosmic-type DP [(b) panel of the figures] given in Table I. When we take into account these parameters values, we chose β in the range of laboratory-type DPs, for which positive and negative solitary potential profiles exist (i.e., for $A \neq 0$). For the cosmic-type DP, only positive solitary potential profiles exist for the whole range of β ranges. It is seen from these figures that W increases with increasing β for both types of plasma. Furthermore, as shown in Fig. 3, W increases (i.e., much wider solitary wave) with α. Figures 4 and 5 show that W decreases (i.e., much narrower solitary wave) with μ_i and σ, for both types of plasma. Finally, according to Eq. (33), W is

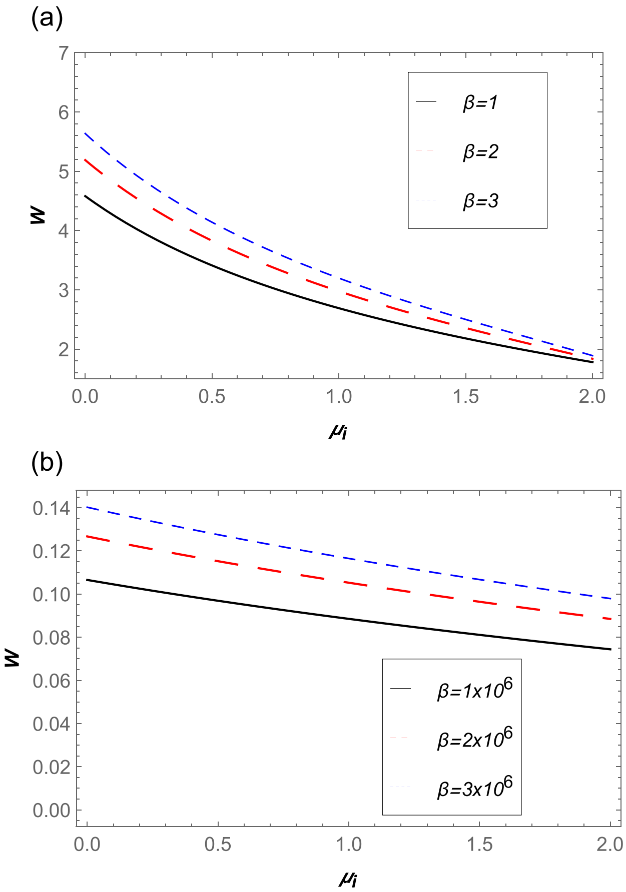

FIG. 4. The variation of the solitary wave width, W, with plasma parameter, $\mu_i\left(\frac{n_{i0}}{z_- n_{-0}}\right)$ for: (a) laboratory-type DP and (b) cosmic-type DP, at different values of $\beta\left(=\frac{m_-}{m_+}\right)$ for the solitary solution represented by Eq. (32).

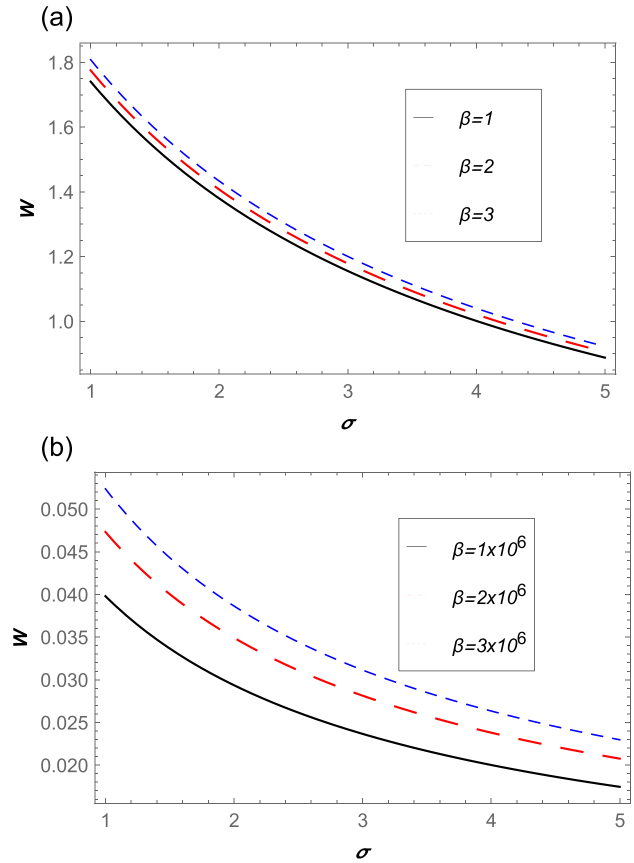

FIG. 5. The variation of the solitary wave width, W, with plasma parameter, $\sigma(=\frac{T_i}{T_e})$ for: (a) laboratory-type DP and (b) cosmic-type DP, at different values of $\beta(=\frac{m_-}{m_+})$ for the solitary solution represented by Eq. (32).

inversely proportional to the square root of the coefficient of the dispersion term, $\sqrt{B}$. Hence, the large W corresponds to lower values of B and hence low dispersion. Since the solitary wave maintains its energy, the lower dispersion is substituted by higher nonlinearity in the plasma system.

V. SUMMARY

In this work, we considered the various travelling wave solutions of two interesting nonlinear evolution equations with variable coefficients (CKP and SKP equations) by using the *GE*-method. These equations describe the basic properties of DAWs in 3D (cylindrical and spherical) geometries which are significantly different from the 1D case.[51] The 1D geometry idealizes the problem and may not be appropriate to describe the real plasma systems either in space or laboratory.[52] On the other hand, the *GE*-method is computerizable and helps us to perform a complicated and tedious algebraic calculation with a computer. Moreover, this method extracts a wide range of travelling wave solutions, some of them are new and interesting. In addition, this method can be used to solve many other nonlinear equations or coupled equations with variable coefficients appearing in plasma physics.

We have applied this analysis to investigate the main characteristics of laboratory and cosmic-type DP systems, consisting of Boltzmann ions, electrons, and inertial positive and negative dust fluids. The evolution of such a system is governed by the nonlinear CKP and SKP evolution equations in cylindrical and spherical coordinates, respectively. We have studied the 3D spatial and temporal behaviors of the obtained solutions of SKP equation and found from the graphs that the profile of the electrostatic potential is divided into compressive sinusoidal, rarefactive sinusoidal, and a periodical explosive or blowup. Some of the obtained solutions have solitonic profile, which results from the balance between nonlinearity and dispersion due to the variations of plasma parameters. It is obvious that the variation of such parameters affects significantly the characteristics of the electrostatic potential.

It should be pointed out that the investigations of this study are helpful to understand salient features of nonlinear behaviour of dusty plasma systems where negative and positive charged dust particulates, as well as, Boltzmann distributed electrons and ions are the major plasma species. Cometary tails, upper mesosphere, Jupiter's magnetosphere[6], even laboratory experiments,[20] etc. are examples of such systems. One of the most interesting phenomena in this regard is the trapping of positively (negatively) charged dust particles by the solitary negative (positive) potential forming larger sized dust particles or being coagulated into extremely large sized neutral dust. This phenomenon may occur in cosmic-type DP systems.[13,22] Hence, our investigations should be helpful to understand the origin of charge separation and dust coagulation in space plasma with positive and negative dust particles.

Finally, it would be noted that the description of DAWs in cylindrical and spherical geometry are more appropriate for investigating plasma systems in laboratory experiments, in fusion reactors and tokamaks, where angular and axial variations in plasma number densities and velocities cannot be ignored. Therefore, this study could be expected to be one of the interesting research topics for future work in this regard.

APPENDIX: GE-METHOD

The NLPDEq with independent variables, R, Θ, φ, and t, and dependent variable ϕ takes the form

$$F(\phi,\phi_t,\phi_R,\phi_\Theta,\phi_\varphi,\phi_{R,\Theta,\varphi},\ldots)=0. \tag{A1}$$

This equation can be solved with the GE-method[42] as follows:

Step 1. We assume that Eq. (A1) has solutions of the form

$$\phi\,(R,\Theta,\varphi,t)=A_0(t)+\sum_{i=0}^{m}A_i\,(t)\,\omega^i(R,\Theta,\varphi,t), \tag{A2}$$

where $\omega(\zeta)$ is the solutions of the following ordinary differential equation (ODE):

$$\frac{d\omega}{d\zeta}=k\sqrt{\sum_{j=4}^{r}c_j\,\omega^j}. \tag{A3}$$

Step 2: We determine the parameter m by balancing the highest order derivative terms with the highest order nonlinear terms in Eq. (A1).

Step3: We substitute Eq. (A2) with Eq. (A3) into Eq. (A1) and equating all terms with the same order of ω^j and $\omega^j\sqrt{\sum_{j=0}^{r}c_j\,\omega^j}$ to zero, then we get a set of over-determined partial differential equations for the differential functions $A_i(t)$ (where $i=0,1,\ldots,n$) and $\zeta(R,\Theta,\varphi,t)[=\alpha(T)R+\beta(T)\varphi+\delta(\Theta,T)T]$.

Step 4. We solve the obtained over-determined partial differential equations by using symbolic computation packages like Mathematica that leads to the explicit expressions for $A_i(t)$ (where $i=1,\ldots,n$) and $\zeta(R,\ \Theta,\ \varphi,\ t)$ or the constraints among them.

Step 5. We consider the case $r=4$ in this paper and hence, Eq. (A2) becomes

$$\omega'=k\sqrt{c_0+c_1\omega+c_2\omega^2+c_3\omega^3+c_4\omega^4}. \tag{A4}$$

This equation admits many kinds of fundamental solutions which may be summarized as follows:[42]

If $c_3=c_1=0$, Eq. (A4) admits

a bell shaped solitary wave solution

$$\omega=k\sqrt{\frac{c_2}{c_4}}\mathrm{sech}\left(\sqrt{c_2}\zeta\right),\quad c_0=0\qquad c_2\succ0,c_4\prec0, \tag{A5}$$

a kink shaped solitary wave solution

$$\omega=k\sqrt{-\frac{c_2}{2c_4}}\tanh\left(\sqrt{-\frac{c_2}{2}}\zeta\right),\quad c_0=\frac{c_2^2}{4c_4}\quad c_2\prec0,c_4\succ0, \tag{A6}$$

two triangular type solutions

$$\omega=k\sqrt{-\frac{c_2}{c_4}}\sec\left(\sqrt{-c_2}\zeta\right),\quad c_0=0\quad c_2<0,c_4\succ0, \tag{A7}$$

$$\omega=k\sqrt{\frac{c_2}{2c_4}}\tan\left(\sqrt{\frac{c_2}{2}}\zeta\right),\quad c_0=\frac{c_2^2}{4c_4}\quad c_2\succ0,c_4\prec0, \tag{A8}$$

a rational type solution

$$\omega=-\frac{k}{\sqrt{c_4}\zeta},\quad c_0=c_2=0,\quad c_4\succ0, \tag{A9}$$

three Jacobi elliptic doubly periodic type solutions

$$\omega=k\sqrt{-\frac{c_2m^2}{c_4(2m^2-1)}}cn\left(\sqrt{\frac{c_2}{(2m^2-1)}}\zeta\right),$$
$$c_4<0,\ c_2>0,\ c_0=-\frac{c_2^2m^2(1-m^2)}{c_4(2m^2-1)}, \tag{A10}$$

$$\omega=k\sqrt{-\frac{c_2}{c_4(2-m^2)}}dn\left(\sqrt{\frac{c_2}{(2-m^2)}}\zeta\right),$$
$$c_4<0,\ c_2>0,\ c_0=-\frac{c_2^2(1-m^2)}{c_4(2-m^2)^2}, \tag{A11}$$

and

$$\omega=k\sqrt{-\frac{c_2m^2}{c_4(m^2+1)}}sn\left(\sqrt{-\frac{c_2}{(m^2+1)}}\zeta\right),$$
$$c_4>0,\ c_2<0,\ c_0=-\frac{c_2^2m^2}{c_4(m^2+1)^2}, \tag{A12}$$

where m is the modulus. The Jacobi elliptic functions possess the following properties:

$$sn^2\zeta+cn^2\zeta=1,\quad dn^2\zeta=1-m^2sn^2\zeta,$$
$$(sn\,\zeta)'=-cn\,\zeta\,dn\,\zeta,\quad (cn\,\zeta)'=sn\,\zeta\,dn\,\zeta,$$
$$(dn\,\zeta)'=-m^2\,sn\,\zeta\,cn\,\zeta.$$

When $m\to0$, the Jacobi elliptic functions degenerate to the triangular functions, i.e.,

$$sn\,\zeta\to\sin\zeta,\quad cn\,\zeta\to\cos\zeta.$$

When $m\to1$, the Jacobi elliptic functions degenerate to the hyperbolic functions, i.e.,

$$sn\,\zeta\to\tanh\zeta,\quad cn\,\zeta\to\sec h\,\zeta.$$

[1]N. N. Rao, P. K. Shukla, and M. Y. Yu, Planet. Space Sci. **38**, 543 (1990).
[2]M. Horànyi and C. K. Goertz, Astrophys. J. **361**, 155 (1990).
[3]M. Horànyi, Annu. Rev. Astron. Astrophys. **34**, 383 (1996).

[4]M. Horányi, G. E. Morfill, and E. Grün, Nature **363**, 144 (1993).
[5]O. Havnes, J. Trøim, T. Blix, W. Mortensen, L. I. Naesheim, E. Thrane, and T. Tønnesen, J. Geophys. Res. **101**, 10839, https://doi.org/10.1029/96JA00003 (1996).
[6]D. A. Mendis and M. Rosenberg, Astron. Astrophys. **32**, 419 (1994).
[7]M. Rosenberg and D. A. Mendis, IEEE Trans. Plasma Sci. **23**, 177 (1995).
[8]A. A. Mamun, Astro Physics. Space Sci. **268**, 443 (1999).
[9]F. Verheest, *Waves Dusty Space Plasmas* (Kluwer, Dordrecht, 2000), Vol. 41, p. 210.
[10]P. K. Shukla and A. A. Mamun, *Introduction to Dusty Plasma Physics* (Institute of Physics, Bristol, 2002), Vol. 8, p. 76.
[11]A. A. Mamun and P. K. Shukla, Geophys. Res. Lett. **29**, 17-1, https://doi.org/10.1029/2002GL015219 (2002).
[12]P. K. Shukla, Phys. Plasmas **10**, 1619 (2003).
[13]F. Sayed and A. A. Mamun, Phys. Plasmas **14**, 014501 (2007).
[14]W. M. Moslem, R. Sabry, and P. K. Shukla, Phys. Plasmas **17**, 032305 (2010).
[15]V. E. Fortovn and G. E. Morfill, *Complex and Dusty Plasmas: From Laboratory to Space* (CRC Press - Taylor & Francis Group, 2010).
[16]S. K. El-Labany, W. F. El-Taibany, and E. E. Behery, Phys. Rev. E **88**, 023108 (2013).
[17]W. F. El-Taibany, Phys. Plasmas **20**, 093701 (2013).
[18]M. M. Selim and U. M. Abdelsalam, Astrophys. Space Sci. **353**, 535 (2014).
[19]A. Barkan, R. L. Merlino, and N. D'Angelo, Phys. Plasmas **2**, 3563 (1995).
[20]A. Barkan, N. D'Angelo, and R. L. Merlino, Planet. Space Sci. **44**, 239 (1996).
[21]O. Havnes, A. Torsten, and A. Brattli, Phys. Scr. **T89**, 133 (2001).
[22]N. D'Angelo, Planet. Space Sci. **49**, 1251 (2001).
[23]W. F. El-Taibany, I. Kourakis, and M. Wadati, Plasma Phys. Controlled Fusion **50**, 074003 (2008).
[24]U. De Angelis, Phys. Scr. **45**(5), 465–474 (1992).
[25]G. L. Delzanno and X. Z. Tang, Phys. Rev. Lett. **113**, 035002 (2014).
[26]M. J. Ablowitz and P. A. Clarkson, *Soliton, Nonlinear Evolution Equations and Inverse Scattering* (Cambridge University Press, New York, 1991).
[27]C. Yan, Phys. Lett. A **77**, 224 (1996).
[28]E. M. E. Zayed, H. A. Zedan, and K. A. Gepreel, Int. J. Nonlinear Sci. Numer. Simul. **5**, 221 (2004).
[29]A. M. Wazwaz, Phys. Lett. A **350**, 367 (2006).
[30]S. K. Liu, Z. T. Fu, S. D. Liu, and Q. Zhao, Phys. Lett. A **289**, 69 (2001).
[31]Z. T. Fu, S. K. Liu, S. D. Liu, and Q. Zhao, Phys. Lett. A **290**, 72 (2001).
[32]E. J. Parkes, B. R. Duffy, and P. C. Abbott, Phys. Lett. A **295**, 280 (2002).
[33]S. Zhang, J. L. Tong, and W. Wang, Phys. Lett. A **372**, 2254 (2008).
[34]S. Reyad, M. M. Selim, A. EL-Depsy, and S. K. El-Labany, J. Nucl. Radiat. Phys. **13**, 1 (2018); available at http://www.afaqscientific.com/jnrp/v13n101.pdf.
[35]H. Alinejad and A. A. Mamun, Phys. Plasmas **18**, 073706 (2011).
[36]W. F. El-Taibany, M. M. Selim, N. A. El-Bedwehy, and O. M. Al-Abbasy, Phys. Plasmas **21**, 073710 (2014).
[37]S. K. Labany, N. A. El-Bedwehy, M. M. Selim, and O. M. Al-Abbasy, Phys. Plasmas **22**, 023711 (2015).
[38]E. E. Behery, M. M. Selim, and W. F. El-Taibany, Phys. Plasmas **22**, 112105 (2015).
[39]M. M. Selim, Astrophys. Space Sci. **361**, 109 (2016).
[40]M. M. Selim, Eur. Phys. J. Plus **131**, 93 (2016).
[41]A. El-Depsy and M. M. Selim, Eur. Phys. J. Plus **131**, 431 (2016).
[42]R. Sabry, M. A. Zahran, and E. Fan, Phys. Lett. A **326**, 93 (2004).
[43]H. Washimi and T. Taniuti, Phys. Rev. Lett. **17**, 996 (1966).
[44]L. Dan, L. X. Guo, and J. T. Li, Phys Plasmas **25**, 013707 (2018).
[45]P. K. Kaw and A. Sen, Phys. Plasmas **5**, 3552 (1998).
[46]P. K. Kaw, Phys Plasmas **8**, 1870 (2001).
[47]S. Garai, S. Jana, M. S. Janaki, and N. Chakrabarti, Europhys. Lett. **114**, 65003 (2016).
[48]H. Ikezi, Phys. Fluids **29**, 1764 (1986).
[49]S. Garai, M. S. Janaki, and N. Chakrabarti, Phys Plasmas **22**, 073706 (2015).
[50]A. M. Wazwaz, *Partial Differential Equations: Methods and Applications* (Balkema Publishers, The Netherlands, 2002).
[51]J. K. Xue, Phys. Lett. A **314**, 479 (2003).
[52]J. R. Franz, P. M. Kintner, and J. S. Pickett, Geophys. Res. Lett. **25**, 1277, https://doi.org/10.1029/98GL50870 (1998).